Journal of the Formosan Medical Association (2016) xx, 1–8

Available online at www.sciencedirect.com

ScienceDirect

journal homepage: www.jfma-online.com

ORIGINAL ARTICLE

Hydration behaviors of calcium silicate-based biomaterials

Yuan-Ling Lee [a,b], Wen-Hsi Wang [c], Feng-Huie Lin [c], Chun-Pin Lin [a,b,d,*]

[a] *Graduate Institute of Clinical Dentistry, School of Dentistry, National Taiwan University Hospital, National Taiwan University, Taipei, Taiwan*
[b] *Department of Dentistry, National Taiwan University Hospital, National Taiwan University, Taipei, Taiwan*
[c] *Institute of Biomedical Engineering, College of Medicine, National Taiwan University, Taipei, Taiwan*
[d] *School of Dentistry, China Medical University and China Medical University Hospital, Taichung, Taiwan, ROC*

Received 6 July 2016; received in revised form 16 July 2016; accepted 20 July 2016

KEYWORDS
calcium silicate;
calcium silicate hydrate;
hydration;
mineral trioxide aggregate

Background/purpose: Calcium silicate (CS)-based biomaterials, such as mineral trioxide aggregate (MTA), have become the most popular and convincing material used in restorative endodontic treatments. However, the commercially available CS-based biomaterials all contain different minor additives, which may affect their hydration behaviors and material properties. The purpose of this study was to evaluate the hydration behavior of CS-based biomaterials with/without minor additives.

Methods: A novel CS-based biomaterial with a simplified composition, without mineral oxides as minor additives, was produced. The characteristics of this biomaterial during hydration were investigated using scanning electron microscopy (SEM), X-ray diffraction (XRD), and Fourier transform infrared (FTIR) spectrometry. The hydration behaviors of commercially available gray and white MTAs with mineral oxide as minor additives were also evaluated for reference.

Results: For all three test materials, the XRD analysis revealed similar diffraction patterns after hydration, but MTAs presented a significant decrease in the intensities of Bi_2O_3-related peaks. SEM results demonstrated similar porous microstructures with some hexagonal and facetted crystals on the outer surfaces. In addition, compared to CS with a simplified composition, the FTIR plot indicated that hydrated MTAs with mineral oxides were better for the polymerization of calcium silicate hydrate (CSH), presenting Si–O band shifting to higher wave numbers, and contained more water crystals within CSH, presenting sharper bands for O–H bending.

Conflicts of interest: The authors have no conflicts of interest relevant to this article.

* Corresponding author.School of Dentistry, China Medical University and China Medical University Hospital, No. 91, Hsueh-Shih Road, Taichung 40402, Taiwan, ROC.
E-mail address: pinlin@ntu.edu.tw (C.-P. Lin).

http://dx.doi.org/10.1016/j.jfma.2016.07.009

Conclusion: Mineral oxides might not result in significant changes in the crystal phases or microstructures during the hydration of CS-based biomaterials, but these compounds affected the hydration behavior at the molecular level.

Introduction

Mineral trioxide aggregate (MTA) is a type of mineral cement developed for restorative endodontic applications.[1] Its excellent sealing ability, good biocompatibility, and induction of hard-tissue regeneration have been supported by many *in vitro* and *in vivo* studies.[2–5] Recent studies have shown that an apatite-like layer forms on the surface of MTA when hydrated in simulated body fluids or phosphate-buffered saline, demonstrating the surface bioactivity of MTA.[6,7] Therefore, MTA has become the most popular and convincing material used in restorative endodontic treatments, including root perforation repair, retrograde filling, apical plug application, and vital pulp therapy. However, MTA requires a long setting time, potentially leading to future complications or even treatment failures. Recently, there have been several attempts to decrease the setting time of MTA using different additives,[8,9] such as Na_2CO_3 and Na_2HPO_4, without understanding the hydration behaviors of MTA.

The original commercially available MTA, approved by the Food and Drug Administration in 1997, is gray (GMTA) in color and primarily comprises tricalcium silicate (C_3S), tricalcium aluminate (C_3A), tetracalcium aluminoferrite (C_4AF), and bismuth oxide (Bi_2O_3). Subsequently, for aesthetic considerations, the GMTA form was modified after adding fluxing agent to remove the colored ingredients, generating a white MTA (WMTA), which was introduced to the market. In addition, the two commercially available MTAs also contain small amounts of additives, such as gypsum ($CaSO_4 \cdot 2H_2O$), MgO, SO_3, Na_2O_3, and K_2O.[10,11] In the cement industry, these minor additives are typically added to adjust the physical properties of Portland cements through effects on the cement hydration. However, the precise mechanism of how these minor additives affect the cement properties during hydration remains unclear.

In this study, to retain the desirable properties of MTAs, a novel calcium silicate (CS) with a simplified composition, containing only C_3S/C_2S, C_3A, and C_4AF, was developed. Because CS has the same major components as commercially available MTAs, except a small amount of minor additives, it would be a good reference material to investigate the hydration mechanism of CS-based biomaterials. The purpose of this study is to evaluate the hydration behaviors of CS-based biomaterials, including CS and the two commercially available MTAs.

Materials and methods

Material preparation

The main components of CS, including Ca_3SiO_5 (C_3S), $Ca_3Al_2O_6$ (C_3A), and $Ca_4Al_2Fe_2O_{10}$ (C_4AF), were prepared by sintering. The raw materials of each component were mixed in a ball mill individually and the substrates with molar ratios were mixed based on the chemical formula of the products. The mixed substrates were subsequently heated to 1400°C for C_3S preparation, 1300°C for C_3A preparation, and 1350°C for C_4AF preparation. The materials were incubated for 2 hours and subsequently quenched in air, followed by milling into powder. The crystal phases of the produced C_3S, C_3A, and C_4AF powders were confirmed through X-ray diffraction (XRD). Based on the ingredients of Type III high-early strength Portland cement, CS was produced after mixing C_3S, C_3A, and C_4AF at a weight ratio of 8:1:1 to mimic commercially available MTAs without minor additives.

Commercially available GMTA (ProRoot MTA; DENTSPLY Tulsa Dental, Johnson City, TN, USA) and WMTA (ProRoot MTA; DENTSPLY Tulsa Dental) were also used for further evaluation in this study.

Microstructure observation

The samples were prepared after mixing the CS powders with distilled water at a weight-to-volume ratio of 2:1, while both MTAs were mixed with distilled water in a weight-to-volume ratio of 3:1, according to the manufacturer's instructions. Subsequently, the mixture was compressed and condensed into a mold. The samples were stored in distilled water at 37°C for 7 days and then removed and air dried overnight at room temperature. The samples were sputter coated with gold using a sputter coater (BIO-RED SC 502; Fisons, Ipswich, UK) and the microstructure of the test materials, including the outer structure (surface structure) and the inner structure (fractured surface), was examined using a scanning electron microscope (SEM; Topcon ABT-60, Tokyo, Japan).

Transformation of hydrated products

The samples were hydrated at 37°C and 100% humidity for 7 days, followed by milling into powder for further evaluations. The crystalline phases of the prepared samples were examined through powder XRD using a Rigaku X-ray powder

Please cite this article in press as: Lee Y-L, et al., Hydration behaviors of calcium silicate-based biomaterials, Journal of the Formosan Medical Association (2016), http://dx.doi.org/10.1016/j.jfma.2016.07.009

diffractometer (Geigerflex; Tokyo, Japan) with an Ni filter and Cu-K_α radiation ($\lambda = 0.154$ nm), generated at 30 kV and 20 mA. The samples were scanned from 10° to 60°, and all data were collected in a continuous scan mode at a scanning rate of 4°/min. Crystalline formations were identified using a computer automatched system with a standard JCPDS data file. The original dry powders of each test material were also analyzed using XRD as a standard to evaluate changes in the crystalline phases of the hydrated products. The characteristics of molecular bonding and functional groups of the prepared samples were determined using a Fourier transform infrared spectrometer (FTIR; JASCO FT/IR-410S spectrometer, Easton, MD, USA) with potassium bromide pellets (KBr, IR grade; Merck, Darmstadt, Germany; samples: KBr = 1:50). The spectra were recorded from 400 cm^{-1} to 4000 cm^{-1}, and 32 scans were recorded each time. Both samples of GMTA and WMTA were prepared for XRD and FTIR analyses.

Results

Scanning electron microscopy analysis of hydrated materials

The results of SEM analysis showed that the hydrated CS and MTAs stored in distilled water had similar outer surface morphologies. Both samples showed porous microstructures with some hexagonal and facetted crystals on the outer surface (Figures 1A–1C). The majority of the porous microstructure was constructed through groundmass with acicular features. Two types of hexagonal crystals embedded in the groundmass were observed: one with a more planar structure (Figures 1A–1C, marked with triangle), and the other with a more pillar-like structure (Figures 1A–1C, marked with arrow). CS exhibited a more planar crystal structure, whereas MTAs exhibited a more pillar-like crystal structure. The SEM image of the fractured surface (Figures 1D–1F) showed that the same type of porous microstructure observed on the surface was also present within both CS and MTA. Interestingly, another type of microstructure was also observed. This type of microstructure was packed as multiple parallel sheets stacked together (multiparallel sheet-layered structure) in various orientations (Figures 1D–1F, marked with star), and some acicular and sheet-like crystals (Figures 1D–1F, marked with hollow arrow) were observed in the pores of the layered structure. High-magnification field emission-SEM (FE-SEM; Figures 2A and 2B) revealed an interstitial space between two sheets, estimated as 50 nm or more. The sheets were generally packed more loosely to the outside and tighter near the center, as illustrated in Figure 2C.

XRD analysis of unhydrated and hydrated materials

The XRD reflection pattern of various materials hydrated in distilled water is shown in Figure 3. For the unhydrated CS sample, several sharp peaks of C_3S ($3CaO \cdot SiO_2$), C_2S

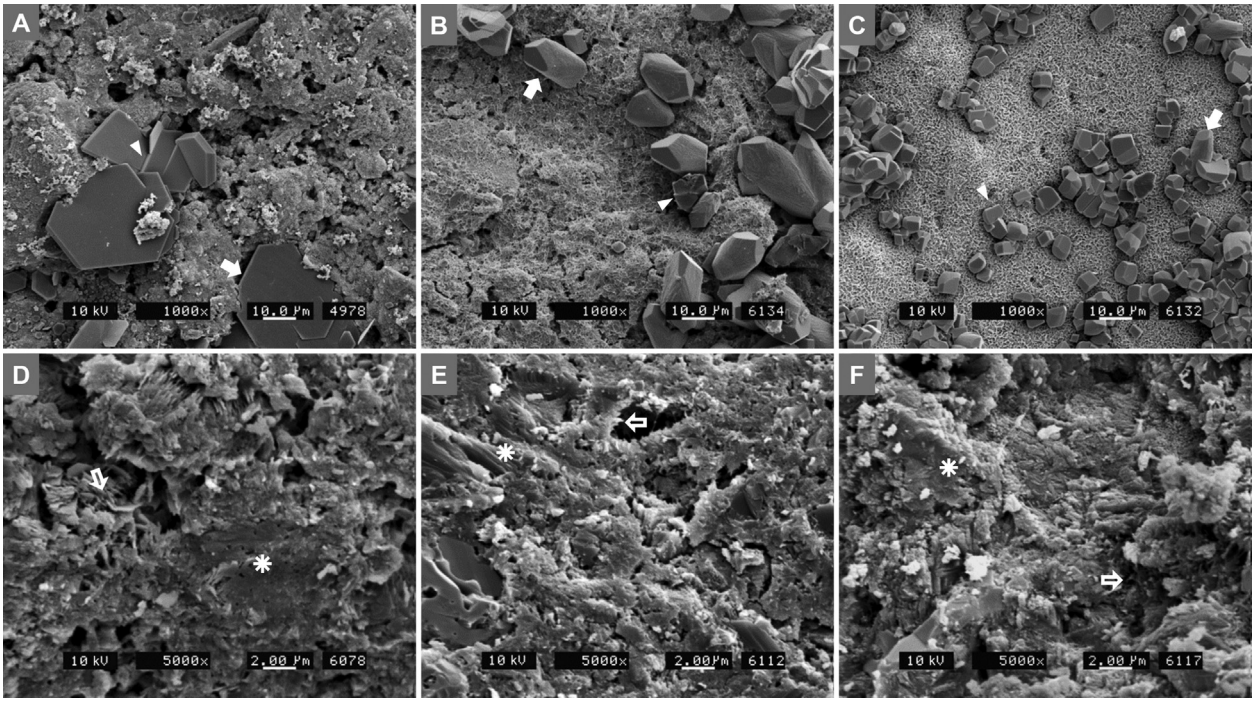

Figure 1 Microstructure of the hydrated calcium silicate (CS)-based biomaterials. Scanning electron microscopy demonstrated the microstructure of CS, gray mineral trioxide aggregate (GMTA), and white MTA (WMTA) after hydration for 7 days. The surface structures of (A) CS, (B) GMTA, and (C) WMTA primarily reflected porous microstructures with acicular crystals, in which some hexagonal (marked with arrow) and facet crystals (marked with triangle) were formed in the interstitial space. On the fractured surface of the hydrated materials, (D) CS, (E) GMTA, and (F) WMTA demonstrated porous structures comprising the layer microstructure with multiple parallel sheets packed together (marked with star), and some acicular and sheet-like crystals (marked with hollow arrow) were observed.

Please cite this article in press as: Lee Y-L, et al., Hydration behaviors of calcium silicate-based biomaterials, Journal of the Formosan Medical Association (2016), http://dx.doi.org/10.1016/j.jfma.2016.07.009

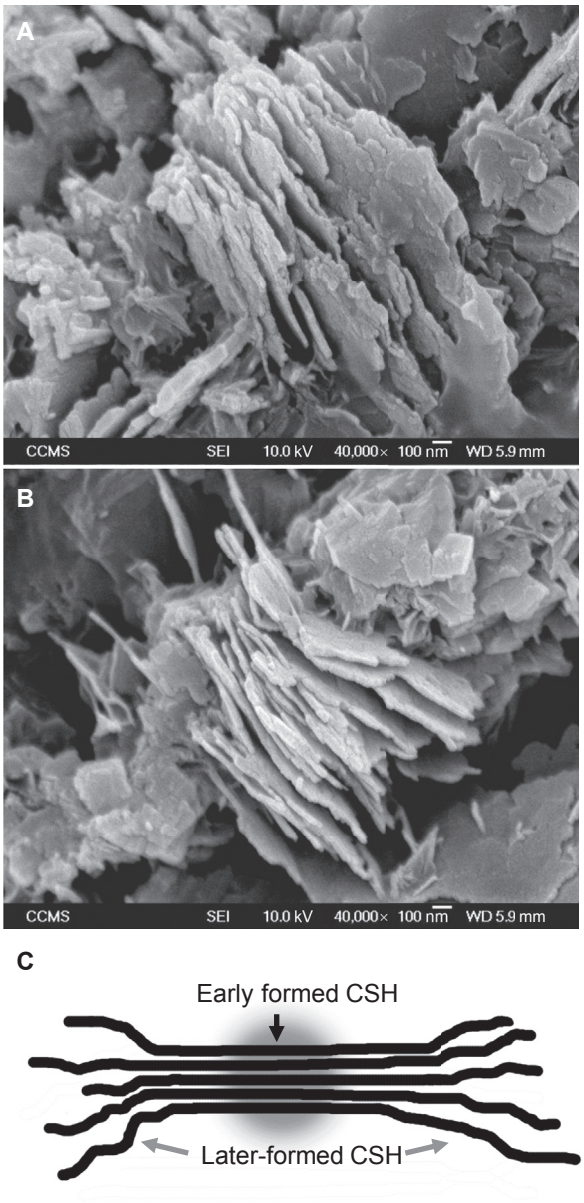

Figure 2 Multilayered nanocrystalline structure of hydrated calcium silicate (CS)-based biomaterials. Field-emission scanning electron microscopy shows the multilayered nanocrystalline structure of (A) hydrated CS and (B) white mineral trioxide aggregate. (C) The illumination demonstrates the multilayered nanocrystalline structure of calcium silicate hydate (CSH), in which the early formed CSH sheets pack together to form nanocrystalline region near the initial nucleation site (indicated by the gray zone) and the latter-formed CSH sheets become more unstructured and disuniformed around the edges of nucleation site.

($2CaO{\cdot}SiO_2$), and C_3A ($3CaO{\cdot}Al_2O_3$) were recorded. Compared with the XRD pattern of unhydrated CS, the decreasing intensity of peaks corresponding to C_3S and C_2S, and new peaks corresponding to portlandite [$Ca(OH)_2$] ($2\theta = 18°$, 34.1°, and 47.1°) and calcite ($CaCO_3$) ($2\theta = 29.6°$ and 48.5°) formation were recorded using XRD (Figure 3). Similar to the XRD diffraction pattern of hydrated CS, the peaks corresponding to portlandite ($2\theta = 18°$) and $CaCO_3$ ($2\theta = 29.6°$) were also observed for hydrated GMTA and WMTA (Figure 3). Compared with the peak intensities of portlandite and $CaCO_3$ from CS, the peak intensities of GMTA and WMTA were lower. Furthermore, there was an obvious decrease in the intensity of the peaks corresponding to Bi_2O_3 ($2\theta = 27.4°$ and 33.1°) after the hydration for both GMTA and WMTA.

Fourier transform infrared spectroscopy analysis of hydrated materials

Figure 4 shows a comparison of the different FTIR plots of the three hydrated test materials. For CS, the absorption bands for H—OH (3055—3550 cm^{-1}) and O—H stretching (3642 cm^{-1} and 2512 cm^{-1}) were observed. The absorption band for CO_3^{-2} ν_2 vibration (875 cm^{-1}) and a broad absorption band for CO_3^{-2} ν_3 vibration (1421 cm^{-1}) were also identified due to calcite formation. The absorption band for Si—O ν_3 asymmetrical stretching was found from 954 cm^{-1} to 960 cm^{-1}.

Unlike CS, various H—OH vibration bands were observed for both MTAs (3195—3613 cm^{-1}). Although the absorption band corresponding to O—H stretching at 3642 cm^{-1} was not present, another absorption band for O—H stretching at a lower wave number was also recorded (GMTA at 2514 cm^{-1}; WMTA at 2512 cm^{-1}). In addition, the absorption band for CO_3^{-2} ν_3 vibration was detected at higher wave numbers for both MTAs (WMTA at 1480 cm^{-1}; GMTA at 1474 cm^{-1}). A broad band for SiO ν_3 vibration was also observed for GMTA (971 cm^{-1}) and WMTA (970 cm^{-1}).

Discussion

According to the studies on Portland cement, the major phases of hydrated C_3S are calcium silicate hydrate (CSH) and calcium hydroxide [$Ca(OH)_2$], which are produced as by-products later during the hydration process.[12,13] CS and the two commercially available MTAs have similar original components, with C_3S as the main original component.[11] Therefore, it was suspected that the hydration of CS and MTAs would primarily be directed through C_3S, which was confirmed based on the SEM of the microstructure. SEM revealed that the main structure of both hydrated CS and MTAs on the external surface exhibited acicular or fibrous crystal formation, similar to the description of the CSH structure in previous studies.[13—16] In the early stage of hydration, the newly formed CSH crystals are acicular or fibrous shaped. As hydration progresses, these CSH crystals form the groundmass.[13,17,18] The hexagonal plate-shaped and hexagonal column-shaped crystals on the surface of CS are most likely $Ca(OH)_2$. However, the facetted crystals are most likely $CaCO_3$, derived from the carbonation of $Ca(OH)_2$ with CO_2 in the atmosphere.[17]

Furthermore, this study was the first to show multilayered nanocrystalline CSH structures using FE-SEM. These unique structures were only observed on the fractured surfaces of the hydrated samples. Based on crystallography, these structures represent different types of CSH crystals formed primarily under the influences of SiO_4 polymerization. As hydration continues, other than the formation of more hydrates, the hydrated SiO_4 monomer in CSH either

Please cite this article in press as: Lee Y-L, et al., Hydration behaviors of calcium silicate-based biomaterials, Journal of the Formosan Medical Association (2016), http://dx.doi.org/10.1016/j.jfma.2016.07.009

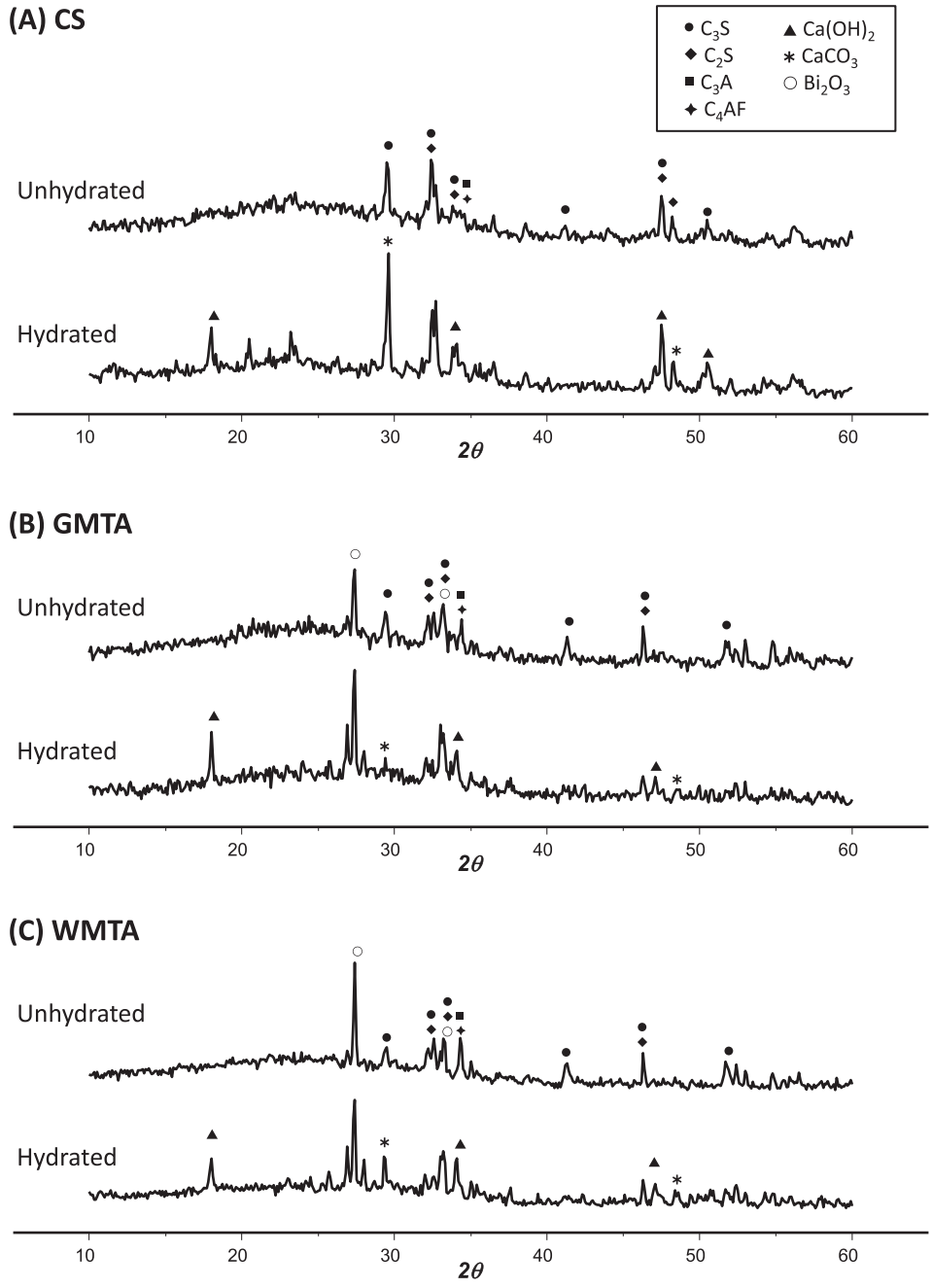

Figure 3 X-ray diffraction (XRD) of unhydrated and hydrated calcium silicate (CS)-based biomaterials. (A) CS biomaterial, (B) gray mineral trioxide aggregate (GMTA), and (C) white MTA (WMTA) presented similar XRD powder patterns, except that the MTAs had Bi_2O_3, which dramatically decreased in intensity after hydration. Both CS and the MTAs presented peaks corresponding to $Ca(OH)_2$ and $CaCO_3$ after hydration.

dimerizes or polymerizes. SiO_4 only crystallizes in a two-dimensional direction, resulting in a flat CSH sheet.[18] The formation of the multilayered structure observed in this study reflected the removal of H_2O from the spaces between the CSH sheets, thereby compacting the sheets.[13,18,19] FE-SEM revealed that the multilayered nanocrystalline structures exhibited a tightly packed central nanocrystalline region with a more disordered outer region, most likely reflecting the limited spaces around the early formed CSH sheets, forcing the sheets at the nucleation site to stack together, forming a more orderly multilayered nanocrystalline region. However, the outer products subsequently formed around the edges of the nucleation site would have extra spaces available, causing a more unstructured and nonuniform growth of the CSH crystals.[20]

Generally, the microstructures of CS, GMTA, and WMTA showed similar morphologies for both the outer surface and the inner structures, suggesting that these three materials might solidify through similar pathways. However, the commercially available MTAs exhibited smaller pore sizes with a more tightly packed multilayered structure

Please cite this article in press as: Lee Y-L, et al., Hydration behaviors of calcium silicate-based biomaterials, Journal of the Formosan Medical Association (2016), http://dx.doi.org/10.1016/j.jfma.2016.07.009

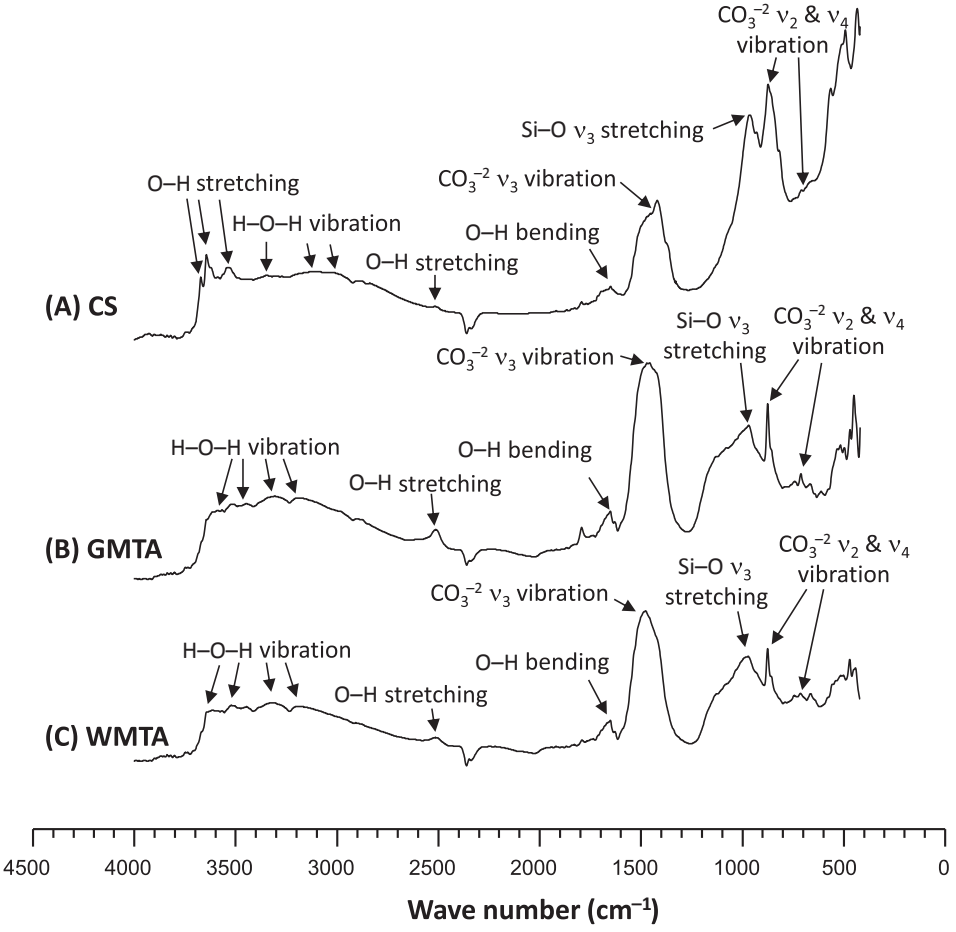

Figure 4 Fourier transform infrared (FTIR) spectra of hydrated calcium silicate (CS)-based biomaterials. FTIR analysis demonstrated the chemical bonding of (A) CS biomaterial, (B) gray mineral trioxide aggregate (GMTA), and (C) white MTA (WMTA). An absorption band for O—H stretching at 3642 cm^{-1} was not detected in both MTAs, but was observed in the CS biomaterial. Additional shifting of Si—O stretching to a higher wave number was observed for the MTAs compared with CS biomaterial.

compared with the microstructure of CS, potentially reflecting the addition of MgO in the MTAs.[11] Less than 1% MgO can induce the formation of the more reactive monoclinic C_3S, instead of the less reactive triclinic C_3S, during the sintering process at high temperatures. The presence of monoclinic C_3S would shorten the time required for the completion of hydration.[21]

Consistently, the XRD analysis demonstrated similar patterns of the crystal phases of the hydrated CS and the two commercially available MTAs, except for the peaks corresponding to bismuth oxide. In addition, the diffraction peaks corresponding to bismuth oxide decreased in intensity in the two commercially available MTAs after hydration, suggesting that bismuth oxide was leached out from the system.[22] Because $Ca(OH)_2$, C_2S, and C_3S present characteristic peaks at $2\theta = 32.1°–34.5°$, the peak at $2\theta = 18°$ was used to identify the production of $Ca(OH)_2$ during hydration. In all three materials, a new peak at $2\theta = 18°$ was observed after hydration, indicating the formation of $Ca(OH)_2$, shown as a hexagonal crystal using SEM. However, the peaks corresponding to the major hydrated product, CSH, were not observed via XRD analysis. This finding most likely reflects the nanoscale crystalline structure of CSH, causing CSH to appear amorphous in XRD.[23,24] Furthermore, unlike the decrease in the intensity of the peaks at $2\theta = 32°–33°$ after hydration, the other peak corresponding to C_3S at $2\theta = 29.6°$, which showed no obvious changes in intensity, was identified through XRD, indicating the formation of $CaCO_3$ after hydration.

Consistent with the XRD results, the FTIR plot demonstrated the appearance of $CaCO_3$, detected as characteristic bands for the CO_3^{-2} group in CS and the two commercially available MTAs. In this study, two techniques, XRD and FTIR, were used to investigate the chemical structure of hydrated CS and the two commercially available MTAs. FTIR detected more differences in the material characteristics among the three test materials after hydration compared with the XRD analysis. The major differences between CS and the two commercially available MTAs in the FTIR plot are the characteristic bands for the O—H group. Both CS and the commercially available MTAs presented bands for H—OH vibration after hydration, indicating the presence of water molecules within the CSH crystals. However, the two commercially available MTAs demonstrated sharper bands for O—H bending compared

Please cite this article in press as: Lee Y-L, et al., Hydration behaviors of calcium silicate-based biomaterials, Journal of the Formosan Medical Association (2016), http://dx.doi.org/10.1016/j.jfma.2016.07.009

with CS, suggesting a higher content of crystal water in the hydrated MTAs.[25]

In addition, a sharp band for O—H stretching at 3642 cm^{-1} was observed in CS, indicating the formation of $Ca(OH)_2$ according to the study of Mollah et al.[26] However, no $Ca(OH)_2$-related O—H bands at 3642 cm^{-1} were detected in the commercially available MTAs. Instead, the MTAs presented a band for O—H stretching at a lower wave number, which may relate to the maturation of crystalline $Ca(OH)_2$. The bands for the O—H groups identified in the commercially available MTAs indicated the formation of $Ca(OH)_2$ with deformed lattices after hydration. From a chemical point of view, the composition of the commercially available MTAs was more complex than that of CS; thus, some lattices of CSH might be substituted with molecules of additives, such as Na_2O_3 or K_2O, contained in MTA during hydration,[11] likely interfering with the O—H stretching and vibration of hydrates, resulting in differences in the FTIR plot.

Using FTIR as a tool to investigate the dynamic changes in Portland cement during hydration, Mollah et al[27] showed shifting of Si—O ν_3 asymmetrical stretching from 930 cm^{-1} to higher wave numbers with time. This shifting was considered as an index of the degree of polymerization of SiO_4^{-4} to SiO_4^{-2} in CSH. Upon hydration, the Si—O bands were eventually shifted to 1138—1155 cm^{-1}.[26] Consistent with the findings of Mollah et al, the shifting of the Si—O ν_3 asymmetrical stretching to higher wave numbers during CS hydration was also identified in this study. According to previous studies,[13,18] the minor components of Portland cement, such as MgO and SO_3, might function as accelerators during hydration. Because commercially available MTAs comprise not only C_3S, C_3A, and C_4AF but also small amounts of MgO and SO_3 compared with CS,[1,11] faster hydration of MTA has been proposed. This statement is supported by the broad bands observed in both hydrated commercially MTAs at 930—1150 cm^{-1} in contrast to the sharp bands detected in hydrated CS centered at 960 cm^{-1}, indicating better CSH polymerization in the commercially available MTAs compared with CS.

In this study, using SEM, XRD, and FTIR as tools, we demonstrated that the minor additives contained in CS-based biomaterials might not generate significant changes in the crystal phases or microstructures during hydration but these did affect the hydration behavior at the molecular level, that is, better polymerization of the hydrated products.

Acknowledgments

The project was supported by grants from Ministry of Science and Technology, R.O.C. (MOST104-2314-B-002-141-MY2). The authors would like to thank Professor Chung-Yuan Mou for assistance with the FE-SEM observations and the Eighth Core Laboratory of Department of Medical Research, National Taiwan University Hospital for technical support.

References

1. Torabinejad M, Chivian N. Clinical applications of mineral trioxide aggregate. *J Endod* 1999;**25**:197—205.
2. Holland R, de Souza V, Murata SS, Nery MJ, Bernabé PF, Otoboni Filho JA, et al. Healing process of dog dental pulp after pulpotomy and pulp covering with mineral trioxide aggregate or Portland cement. *Braz Dent J* 2001;**12**:109—13.
3. Lee SJ, Monsef M, Torabinejad M. Sealing ability of a mineral trioxide aggregate for repair of lateral root perforations. *J Endod* 1993;**19**:541—4.
4. Osorio RM, Hefti A, Vertucci FJ, Shawley AL. Cytotoxicity of endodontic materials. *J Endod* 1998;**24**:91—6.
5. Torabinejad M, Hong CU, Pitt Ford TR, Kettering JD. Cytotoxicity of four root end filling materials. *J Endod* 1995;**21**:489—92.
6. Reyes-Carmona JF, Felippe MS, Felippe WT. The biomineralization ability of mineral trioxide aggregate and Portland cement on dentin enhances the push-out strength. *J Endod* 2010;**36**:286—91.
7. Qi YP, Li N, Niu LN, Primus CM, Ling JQ, Pashley DH, et al. Remineralization of artificial dentinal caries lesions by biomimetically modified mineral trioxide aggregate. *Acta Biomater* 2012;**8**:836—42.
8. Huan Z, Chang J. Effect of sodium carbonate solution on self-setting properties of tricalcium silicate bone cement. *J Biomater Appl* 2008;**23**:247—62.
9. Lotfi M, Vosoughhosseini S, Saghiri MA, Mesgariabbasi M, Ranjkesh B. Effect of white mineral trioxide aggregate mixed with disodium hydrogen phosphate on inflammatory cells. *J Endod* 2009;**35**:703—5.
10. Torabinejad M, Watson TF, Pitt Ford TR. Sealing ability of a mineral trioxide aggregate when used as a root end filling material. *J Endod* 1993;**19**:591—5.
11. Torabinejad M, White DJ. Tooth filling material and method of use. US Patent 5415547. Loma Linda, CA; Loma Linda University; 1995.
12. Brown PW, Hellmann JR, Klimkiewicz M. Examples of evolution of microstructure in ceramics and composites. *Microsc Res Tech* 1993;**25**:474—86.
13. Bye GC. *Portland cement: composition, production, and properties*. New York: Pergamon Press; 1983.
14. Lawrence Jr FV, Young JF. Studies on the hydration of tricalcium silicate pastes I. Scanning electron microscopic examination of microstructural features. *Cem Concr Res* 1973;**3**:149—61.
15. Kjellsen KO, Lagerblad B. Microstructure of tricalcium silicate and Portland cement systems at middle periods of hydration-development of Hadley grains. *Cem Concr Res* 2007;**37**:13—20.
16. Camilleri J. Characterization and hydration kinetics of tricalcium silicate cement for use as a dental biomaterial. *Dent Mater* 2011;**27**:836—44.
17. Häußler F, Palzer S, Angela E. Nondestructive microstructural investigations on hydrating cement paste and tricalcium silicate by small angle neutron scattering. In: *Leipzig annual civil engineering report*, vol. 4. Leipzig: Universität Leipzig, Institut für Massivbau und Baustofftechnologie, Wirtschaftswissenschaftliche Fakultät; 1999. p. 47—64.
18. Bentur A. Cementitious materials-nine millennia and a new century: past, present and future. *J Mater Civil Eng* 2002;**14**:2—22.
19. Brown PW. Hydration behavior of calcium phosphates is analogous to hydration behavior of calcium silicates. *Cem Concr Res* 1999;**29**:1167—71.
20. Gartner EM. A proposed mechanism for the growth of C-S-H during the hydration of tricalcium silicate. *Cem Concr Res* 1997;**27**:665—72.
21. Katyal NK, Ahluwalia SC, Parkash R. Solid solution and hydration behavior of magnesium-bearing tricalcium silicate phase. *Cem Concr Res* 1998;**28**:867—75.
22. Formosa LM, Mallia B, Bull T, Camilleri J. The microstructure and surface morphology of radiopaque tricalcium silicate

cement exposed to different curing conditions. *Dent Mater* 2012;**28**:584–95.
23. Gauffinet S, Finot E, Lesniewska E, Nonat A. Direct observation of the growth of calcium silicate hydrate on alite and silica surface by atomic force microscopy. *Earth Planet Sci* 1998; **327**:231–6.
24. Nonat A. The structure and stoichiometry of C-S-H. *Cem Concr Res* 2004;**34**:1521–8.
25. Guerrero A, Goni S. Microstructure and mechanical performance of belite cements from high calcium coal fly ash. *J Am Ceram Soc* 2005;**88**:1845–53.
26. Mollah MYA, Yu W, Schennach R, Cocke DLA. Fourier transform infrared spectroscopic investigation of the early hydration of Portland cement and the influence of sodium lignosulfonate. *Cem Concr Res* 2000;**30**:267–73.
27. Mollah MYA, Lu F, Cocke DL. An X-ray diffraction and Fourier transform infrared spectroscopic characterization of the speciation of arsenic (V) in Portland cement type V. *Sci Total Environ* 1998;**224**:57–68.

Please cite this article in press as: Lee Y-L, et al., Hydration behaviors of calcium silicate-based biomaterials, Journal of the Formosan Medical Association (2016), http://dx.doi.org/10.1016/j.jfma.2016.07.009